Anisotropic Mesh Adaptation for Solution of Finite Element Problems Using Hierarchical Edge-Based Error Estimates

Abdellatif Agouzal[1], Konstantin Lipnikov[2], and Yuri Vassilevski[3]

[1] Universite de Lyon 1, Laboratoire d'Analyse Numerique
agouzal@univ-lyon1.fr
[2] Los Alamos National Laboratory, Theoretical Division
lipnikov@lanl.gov
[3] Institute of Numerical Mathematics
yuri.vassilevski@gmail.com

Abstract. We present a new technology for generating meshes minimizing the interpolation and discretization errors or their gradients. The key element of this methodology is construction of a space metric from edge-based error estimates. For a mesh with N_h triangles, the error is proportional to N_h^{-1} and the gradient of error is proportional to $N_h^{-1/2}$ which are the optimal asymptotics. The methodology is verified with numerical experiments.

1 Introduction

Unstructured simplicial meshes are ideally suited for adaptive finite element calculations. The simplexes can be aligned with solution features and cover the computational domain in an optimal way to equidistribute the error. This results in a smaller computational mesh and potentially faster calculations.

Generation of optimal adaptive meshes requires error estimates or error indicators that carry directional information about the solution. In this article, we use error estimates that are associated with mesh edges. We consider edge-based error estimates for the interpolation error and hierarchical error estimates for the discretization error [12]. In both cases, we employ the methodology developed in [1, 3, 4] for the interpolation error. This methodology results in a metric that captures correctly isotropic and anisotropic solution features. Here, we continue analysis of this metric, in particular, its smoothness and anisotropic alignment.

Other methods for generating a space metric are often based on the Hessian of the discrete solution [18, 15, 14, 13]. For such a metric, optimal error estimates for the interpolation error have been proved in [2, 8, 14, 17, 18]. The Hessian-based metric has been successfully applied to adaptive solution of PDEs [7, 13, 15]. However, its theoretical analysis requires to make an additional assumption that the discrete Hessian approximates the continuous one in the maximum norm. Despite the fact that this assumption is frequently

violated in many Hessian recovery methods, the generated adaptive meshes still result in optimal error reduction.

The technology, which we proposed in [1, 3, 4] does not require the aforementioned approximation assumption. It can be also applied to adaptive solution of various finite element problems including problems with discontinuous finite element solutions. The price to pay is that error estimates or error indicators have to be prescribed to mesh edges. The finite element literature provides a number of ways to obtain these error estimates. For instance, in CFD literature, edge-based error estimates have appeared occasionally since mid of 1990's but have not received adequate theoretical treatment [5, 6]. In this article, we use the hierarchical error estimates from [12] and provide a numerical analysis of our methodology for the adaptive solution of finite element problems. The cornerstone of this methodology is construction of a space metric from edge-based error estimates.

We define a tensor metric $\mathfrak{M}$ such that the volume and the perimeter of a simplex measured in this metric control the norm of error or its gradient. The equidistribution principle, which can be traced back to D'Azevedo [11], suggests to balance $\mathfrak{M}$-volumes and $\mathfrak{M}$-perimeters. This leads to meshes that are quasi-uniform in the piecewise constant metric $\mathfrak{M}$. The piecewise constant metric may produce instabilities in an adaptive process, especially when the length of a mesh edge, measured in all metrics associated with simplexes sharing the edge, varies strongly. We show numerically that this variation is relatively small for our piecewise constant metrics. This allows us to convert the piecewise constant metric into a continuous one for additional robustness of the adaptive process.

A piecewise constant tensor metric that controls the error is not unique. Any such metric results in asymptotically optimal reduction of the error [1]. In this paper, we show how to build a metric that preserves solution anisotropy. The resulting quasi-optimal mesh equidistributes both the error over simplexes and the maximum norm of the error over edges of each simplex.

The paper outline is as follows. In Section 2, we derive metrics optimal for the interpolation errors. In Section 3, we present the algorithm for generating adaptive meshes. In Section 4, we apply the methodology for adaptive solution of finite element problems.

2 Interpolation Error Analysis

2.1 Edge-Based Error Estimates and a Tensor Metric

Let $\Omega \subset \Re^d$ be a bounded polyhedral domain and Ω_h be a conformal simplicial mesh with N_h simplexes. Let $\mathfrak{M}$ be a piecewise constant tensor metric on Ω_h. The volume of simplex Δ and the length of edge $\mathbf{e}$ in this metric are denoted by $|\Delta|_{\mathfrak{M}}$ and $|\mathbf{e}|_{\mathfrak{M}}$, respectively [2]. The total length of all edges of simplex Δ in denoted by $|\partial\Delta|_{\mathfrak{M}}$. We shall refer to $|\partial\Delta|_{\mathfrak{M}}$ as the perimeter of Δ in the metric $\mathfrak{M}$.

Let $\mathcal{I}_1 u$ be the piecewise linear Lagrange interpolant of u, and $\mathcal{I}_{1,\Delta} u$ be its restriction to Δ. Similarly, let $\mathcal{I}_2 u$ be the piecewise quadratic Lagrange interpolant of u, and $\mathcal{I}_{2,\Delta} u$ be its restriction to Δ. Our goal is to generate a mesh that minimizes (approximately) the L^p-norm, $p \in (0, \infty]$, of the interpolation error

$$e = u - \mathcal{I}_1 u$$

or its gradient ∇e. A sequence of meshes with increasing number of simplexes must provide the optimal reduction of this error. For instance, the Tichomirov result [16] implies that the optimal reduction of the L^∞-norm of error is proportional to N_h^{-1}.

Let us consider a particular d-simplex Δ with vertices $\mathbf{v}_i$, $i = 1, \ldots, d+1$, edge vectors $\mathbf{e}_k = \mathbf{v}_i - \mathbf{v}_j$, $1 \le i < j \le d+1$, and mid-edge points $\mathbf{c}_k$, $k = 1, \ldots, n_d$, where $n_d = d(d+1)/2$. Let λ_i, $i = 1, \ldots, d+1$, be the linear functions on Δ such that $\lambda_i(\mathbf{v}_j) = \delta_{ij}$ where δ_{ij} is the Kronecker symbol. For every edge $\mathbf{e}_k$, we define the quadratic bubble function $b_k = \lambda_i \lambda_j$.

Let u be a continuous function and $u_2 = \mathcal{I}_{2,\Delta}\, u$ be its quadratic approximation on Δ. We have

$$e_2 = u_2 - \mathcal{I}_{1,\Delta} u_2 = 4 \sum_{k=1}^{n_d} (u_2(\mathbf{c}_k) - \mathcal{I}_{1,\Delta} u_2(\mathbf{c}_k))\, b_k \equiv \sum_{k=1}^{n_d} \gamma_k\, b_k. \tag{1}$$

The L^2-norm of the error e_2 is given by

$$\|e_2\|^2_{L^2(\Delta)} = |\Delta|\, (\mathbb{B}\, \boldsymbol{\gamma}, \boldsymbol{\gamma}), \tag{2}$$

where $\boldsymbol{\gamma}$ is a vector with n_d components γ_k and $\mathbb{B}$ is the $n_d \times n_d$ symmetric positive definite scaled Gramm matrix with positive entries $\mathbb{B}_{k,l} = |\Delta|^{-1} \int_\Delta b_k b_l \,\mathrm{d}V$. Note that (2) is only a number; therefore, it does not provide any directional information. To recover this information, we split the error into n_d pieces associated with edges of Δ:

$$\|e_2\|_{L^2(\Delta)} = |\Delta|^{1/2} \sum_{k=1}^{n_d} \alpha_k \qquad \text{and} \qquad \sum_{k=1}^{n_d} \alpha_k = (\mathbb{B}\boldsymbol{\gamma}, \boldsymbol{\gamma})^{1/2}. \tag{3}$$

Not careful selection of α_k may result in loss of directional information. In the sequel, we motivate the following choice of α_k:

$$\alpha_k = |\gamma_k|\, (\mathbb{B}\boldsymbol{\gamma}, \boldsymbol{\gamma})^{1/2} \left(\sum_{k=1}^{n_d} |\gamma_k| \right)^{-1}. \tag{4}$$

We repeat the above derivations for the gradient of the error. The L^2-norm of ∇e_2 is given by

$$\|\nabla e_2\|^2_{L^2(\Delta)} = \| \sum_{k=1}^{n_d} \gamma_k \nabla b_k \|^2_{L^2(\Delta)} = |\Delta| (\widetilde{\mathbb{B}}\, \boldsymbol{\gamma}, \boldsymbol{\gamma}),$$

where $\widetilde{\mathbb{B}}$ is the $n_d \times n_d$ symmetric positive definite matrix with entries $\widetilde{\mathbb{B}}_{k,l} = |\Delta|^{-1} \int_\Delta \nabla b_k \cdot \nabla b_l \, \mathrm{d}V$. Again, we split this error (a number) into n_d edge-based error estimates $\tilde{\alpha}_k \geq 0$ such that

$$\|\nabla e_2\|^2_{L^2(\Delta)} = |\Delta| \sum_{k=1}^{n_d} \tilde{\alpha}_k \qquad \text{and} \qquad \sum_{k=1}^{n_d} \tilde{\alpha}_k = (\widetilde{\mathbb{B}}\,\boldsymbol{\gamma}, \boldsymbol{\gamma}). \tag{5}$$

Again, a proper choice of α_k is required to preserve directional information in a final metric. In the sequel, we motivate the following choice of $\tilde{\alpha}_k$:

$$\tilde{\alpha}_k = |\gamma_k| \, (\widetilde{\mathbb{B}}\,\boldsymbol{\gamma}, \boldsymbol{\gamma}) \left(\sum_{k=1}^{n_d} |\gamma_k| \right)^{-1}. \tag{6}$$

In both cases, the edges-based errors α_k and $\tilde{\alpha}_k$ are proportional to $|\gamma_k|$ which is the same for all simplexes sharing the edge $\mathbf{e}_k$. This observation is a key to understanding 'smoothness' of the metric whose element-by-element construction is based on the following result [1, 4].

Lemma 1. *Let α_k, $k = 1, \ldots, n_d$, be values prescribed to edges of a d-simplex Δ such that*

$$\alpha_k \geq 0 \qquad \textit{and} \qquad \sum_{k=1}^{n_d} \alpha_k > 0.$$

Then, there exists a constant tensor metric $\mathfrak{M}_\Delta$ such that

$$\left(\frac{d!}{(d+1)(d+2)} \right)^{1/d} |\Delta|^{2/d}_{\mathfrak{M}_\Delta} \leq \sum_{k=1}^{n_d} \alpha_k \leq |\partial\Delta|^2_{\mathfrak{M}_\Delta}. \tag{7}$$

The proof [1, 4] of Lemma 1 provides the constructive way to define the metric $\mathfrak{M}_\Delta$. Due to its importance, we present a shortened proof here.

Proof. Let us define the quadratic function

$$v_2 = -\frac{1}{2} \sum_{k=1}^{n_d} \alpha_k b_k.$$

The trace of v_2 on $\mathbf{e}_k$ is a quadratic function w_2 vanishing at endpoints $\mathbf{v}_i$, $\mathbf{v}_j$ of $\mathbf{e}_k$ with an extremum at $\mathbf{c}_k$. Therefore, $w_2'(\mathbf{c}_k) = 0$ and $\nabla v_2(\mathbf{c}_k) \cdot \mathbf{e}_k = 0$. Let $\mathbb{H}$ be the Hessian of v_2. Applying the multi-point Taylor formula [9, 10] for v_2 at endpoints $\mathbf{v}_i$ and $\mathbf{v}_j$ of $\mathbf{e}_k$, we get

$$\begin{aligned} 0 = v_2(\mathbf{v}_i) &= v_2(\mathbf{c}_k) - \frac{1}{2} \nabla v_2(\mathbf{c}_k) \cdot \mathbf{e}_k + \frac{1}{8} (\mathbb{H}\,\mathbf{e}_k, \mathbf{e}_k), \\ 0 = v_2(\mathbf{v}_j) &= v_2(\mathbf{c}_k) + \frac{1}{2} \nabla v_2(\mathbf{c}_k) \cdot \mathbf{e}_k + \frac{1}{8} (\mathbb{H}\,\mathbf{e}_k, \mathbf{e}_k). \end{aligned} \tag{8}$$

Thus,

$$(\mathbb{H}\,\mathbf{e}_k, \mathbf{e}_k) = \alpha_k.$$

The Hessian $\mathbb{H}$ may be indefinite and hence cannot be used to define the metric $\mathfrak{M}_\Delta$. In order to make it positive semidefinite, we take its spectral module:

$$|\mathbb{H}| = W^T |\Lambda|\, W,$$

where $\mathbb{H} = W^T \Lambda W$ is the spectral decomposition of the symmetric matrix $\mathbb{H}$.

If $\det\mathbb{H} \neq 0$, we set $\mathfrak{M}_\Delta = |\mathbb{H}|$. The upper bound follows from

$$|\partial\Delta|^2_{|\mathbb{H}|} = \left(\sum_{k=1}^{n_d} (|\mathbb{H}|\mathbf{e}_k, \mathbf{e}_k)^{1/2}\right)^2 \geq \sum_{k=1}^{n_d} (|\mathbb{H}|\mathbf{e}_k, \mathbf{e}_k) \geq \sum_{k=1}^{n_d} |(\mathbb{H}\,\mathbf{e}_k, \mathbf{e}_k)| = \sum_{k=1}^{n_d} \alpha_k.$$

To estimate the lower bound, we use formula for the Cayley-Menger determinant generalized to the case $\mathbb{H} \neq \mathbb{I}$ (for its proof we refer to [1]):

$$\det(\mathbb{H})\,|\Delta|^2 = \frac{(-1)^{d-1}}{2^d (d!)^2} \det(K(\mathbb{H})), \tag{9}$$

where

$$K(\mathbb{H}) = \begin{pmatrix} (\mathbb{H}\mathbf{v}_{11}, \mathbf{v}_{11}) & \cdots & (\mathbb{H}\mathbf{v}_{1d_1}, \mathbf{v}_{1d_1}) & 1 \\ \vdots & \ddots & \vdots & \vdots \\ (\mathbb{H}\mathbf{v}_{d_1 1}, \mathbf{v}_{d_1 1}) & \cdots & (\mathbb{H}\mathbf{v}_{d_1 d_1}, \mathbf{v}_{d_1 d_1}) & 1 \\ 1 & \cdots & 1 & 0 \end{pmatrix} \tag{10}$$

and $\mathbf{v}_{ij} \equiv \mathbf{v}_i - \mathbf{v}_j$. Therefore,

$$\begin{aligned} |\Delta|^2_{|\mathbb{H}|} = \det(|\mathbb{H}|)\,|\Delta|^2 &= \frac{(-1)^{d-1}}{2^d (d!)^2} \det(K(|\mathbb{H}|)) \\ &\leq \frac{1}{2^d (d!)^2} \sup_{\boldsymbol{\alpha} \in \Re^{n_d}} \frac{|\det K(\mathbb{H})|}{\max\limits_{1 \leq k \leq n_d} \alpha_k^d} \left(\sum_{k=1}^{n_d} \alpha_k\right)^d. \end{aligned} \tag{11}$$

For a square matrix $K(\mathbb{H})$ with elements $k_{i,j}$, it holds

$$|\det(K(\mathbb{H}))| \leq |\sum_{\boldsymbol{\sigma}} \prod_{i=1}^{d+2} k_{i,\sigma_i}| \leq (d+2)!\, \max_{\boldsymbol{\sigma}} |\prod_{i=1}^{d+2} k_{i,\sigma_i}|,$$

where the summation is performed over all possible permutations $\boldsymbol{\sigma}$ of matrix rows and columns. Since $k_{i,j} = (\mathbb{H}\,\mathbf{e}_k, \mathbf{e}_k) = \alpha_k$, $1 \leq i < j \leq d_1$, from (10) we derive that $\det(K(\mathbb{H}))$ is a homogeneous polynomial of degree d of α_k and

$$\sup_{\boldsymbol{\alpha} \in \Re^{n_d}} \frac{|\det K(\mathbb{H})|}{\max\limits_{1 \leq k \leq n_d} \alpha_k^d} \leq (d+2)! \sup_{\boldsymbol{\alpha} \in \Re^{n_d}} \frac{\max\limits_{1 \leq k \leq n_d} \alpha_k^d}{\max\limits_{1 \leq k \leq n_d} \alpha_k^d} \leq (d+2)!\,.$$

Therefore, we conclude from (11) that

$$|\Delta|^2_{|\mathbb{H}|} \le \frac{1}{2^d}\frac{(d+1)(d+2)}{d!}\left(\sum_{k=1}^{n_d}\alpha_k\right)^d$$

which implies the lower bound in (7).

If $\det(\mathbb{H}) = 0$, the Hessian $\mathbb{H}$ cannot be used to generate a metric. In this case, we *modify* α_k to get a new quadratic function v_2 with a non-degenerate Hessian such that (7) is still satisfied. For the sake of simplicity, we restrict ourselves to the case $0 \le \alpha_1 \le \alpha_2 \le \cdots \le \alpha_{n_d}$ and $\alpha_{n_d} \ne 0$. The modified edge data are

$$\tilde\alpha_k = \alpha_k, \quad k = 1, \ldots, n_d - 1, \qquad \tilde\alpha_{n_d} = (1+\delta)\alpha_{n_d},$$

where $\delta \in]0, 1]$.

Let $\tilde v_2(\delta) = -\frac{1}{2}\sum_{k=1}^{n_d}\tilde\alpha_k b_k$ be the modified quadratic function and $\widetilde{\mathbb{H}}(\delta)$ be its Hessian. Formulas (9) and (10) imply that $p(\delta) \equiv \det(\widetilde{\mathbb{H}}(\delta))$ is a polynomial of degree two. Since $p(0) = \det(\mathbb{H}) = 0$, there exists $\delta_0 \in]0, 1]$ such that $\det(\widetilde{\mathbb{H}}(\delta_0)) \ne 0$. We set $\mathfrak{M}_\Delta = |\widetilde{\mathbb{H}}(\delta_0)|$ and check that

$$\sum_{k=1}^{n_d}\alpha_k \le \sum_{k=1}^{n_d}\tilde\alpha_k \le \sum_{k=1}^{n_d}(|\widetilde{\mathbb{H}}(\delta_0)|\mathbf{e}_k, \mathbf{e}_k) \le \left(\sum_{k=1}^{n_d}(|\widetilde{\mathbb{H}}(\delta_0)|\mathbf{e}_k, \mathbf{e}_k)^{1/2}\right)^2 = |\partial\Delta|^2_{\mathfrak{M}_\Delta}$$

and

$$\sum_{k=1}^{n_d}\alpha_k \ge \frac{1}{2}\sum_{k=1}^{n_d}\tilde\alpha_k \ge \left(\frac{(d+1)(d+2)}{d!}\right)^{-\frac{1}{d}}|\Delta|^{\frac{2}{d}}_{\mathfrak{M}_\Delta}.$$

This proves the assertion of the lemma. □

Using Lemma 1 and norm definition (3), we build the auxiliary metric $\mathfrak{M}_\Delta$ for error e_2. Similarly, using Lemma 1 and norm definition (5), we build the auxiliary metric $\widetilde{\mathfrak{M}}_\Delta$ for ∇e_2. These metrics do not provide a geometric representation of the error since the error estimates involve also the volume of simplex in the Cartesian metric. This mismatch is fixed in the following section.

2.2 Metrics for the L^p-norm of Error and Its Gradient

In this section, we consider L^p-norms, $p \ge 1$, of the errors as well as L^p-quasi-norms, $0 < p < 1$. As described in [18, 1, 4], as well as in [14], the metrics controlling various L^p-norms differ by a scaling factor. Let

$$\mathfrak{M}_{\Delta,p} = (\det(\mathfrak{M}_\Delta))^{-1/(d+2p)}\,\mathfrak{M}_\Delta \quad \text{and} \quad \widetilde{\mathfrak{M}}_{\Delta,p} = (\det(\widetilde{\mathfrak{M}}_\Delta))^{-1/(d+p)}\widetilde{\mathfrak{M}}_\Delta.$$

The following estimates are proved in [18, 1, 4].

Lemma 2. *Let $\mathfrak{M}_{\Delta,p}$ and $\widetilde{\mathfrak{M}}_{\Delta,p}$ be the constant tensor metrics defined above. Then,*

$$c_p|\Delta|^{2/d+1/p}_{\mathfrak{M}_{\Delta,p}} \le \|e_2\|_{L^p(\Delta)} \le C_p\,|\Delta|^{1/p}_{\mathfrak{M}_{\Delta,p}}\,|\partial\Delta|^2_{\mathfrak{M}_{\Delta,p}} \tag{12}$$

and

$$\tilde{c}_p|\Delta|^{1/d+1/p}_{\widetilde{\mathfrak{M}}_{\Delta,p}} \le \|\nabla e_2\|_{L^p(\Delta)} \le \tilde{C}_p\,|\Delta|^{1/p}_{\widetilde{\mathfrak{M}}_{\Delta,p}}\,|\partial\Delta|_{\widetilde{\mathfrak{M}}_{\Delta,p}}, \tag{13}$$

where constants c_p, C_p, $\tilde{c}_p$, $\tilde{C}_p$ depend only on d and p.

For brevity, we confine ourselves to the case $p = \infty$. In this case, the constants in Lemma 2 depend only on d. Moreover, the metrics generated by Lemma 1 are optimal, i.e. $\mathfrak{M}_{\Delta,\infty} = \mathfrak{M}_\Delta$ and $\widetilde{\mathfrak{M}}_{\Delta,\infty} = \widetilde{\mathfrak{M}}_\Delta$.

2.3 Extension to General Functions

For a given continuous function u, we use the computable error e_2 to estimate the true error e:

$$e = u - \mathcal{I}_{1,\Delta}u.$$

Let $\mathcal{F}$ be the space of symmetric $d \times d$ matrices and $|\mathbb{H}|$ be the spectral module of $\mathbb{H} \in \mathcal{F}$. We introduce the following notations:

$$|||\mathbf{e}_k|||^2_{|\mathbb{H}|} = \max_{\mathbf{x}\in\Delta}\left(|\mathbb{H}(\mathbf{x})|\,\mathbf{e}_k, \mathbf{e}_k\right) \qquad \text{and} \qquad |||\partial\Delta|||^2_{|\mathbb{H}|} = \sum_{k=1}^{n_d} |||\mathbf{e}_k|||^2_{|\mathbb{H}|}.$$

The following result is proved in [1, 4].

Lemma 3. *Let $u \in C^2(\bar{\Delta})$. Then,*

$$\frac{d+1}{2d}\|e_2\|_{L^\infty(\Delta)} \le \|e\|_{L^\infty(\Delta)} \le \|e_2\|_{L^\infty(\Delta)} + \frac{1}{4}\inf_{\mathbb{F}\in\mathcal{F}} |||\partial\Delta|||^2_{|\mathbb{H}-\mathbb{F}|}.$$

and

$$\|\nabla e_2\|_{L^\infty(\Delta)} - \mathrm{osc}(\mathbb{H},\Delta) \le \|\nabla e\|_{L^\infty(\Delta)} \le \|\nabla e_2\|_{L^\infty(\Delta)} + \mathrm{osc}(\mathbb{H},\Delta), \tag{14}$$

where the oscillation term is

$$\mathrm{osc}(\mathbb{H},\Delta) = C_{osc}\frac{|\partial\Delta|^{d-1}}{|\Delta|}\inf_{\mathbb{F}\in\mathcal{F}} |||\partial\Delta|||^2_{|\mathbb{H}-\mathbb{F}|}$$

and C_{osc} depends only on d.

The oscillation terms are conventional in the contemporary error analysis. Their value depend on the simplex and particular features of the function. For smooth solutions and shape-regular simplexes, the oscillation terms are much smaller than the error value.

2.4 On Selection of α_k

Let $\mathbb{H}(u_2)$ be definite. The derivation of metric $\mathfrak{M}_\Delta$ suggests a simple motivation for the choices (4) and (6). Since the bubble function b_k is non-zero only on one edge, we get

$$|(\mathfrak{M}_\Delta \mathbf{e}_k, \mathbf{e}_k)| = -\frac{1}{2}\alpha_k(\mathbb{H}(b_k)\mathbf{e}_k, \mathbf{e}_k).$$

The last term is the second derivative in direction $\mathbf{e}_k$. The inner product is a constant independent of the edge length and shape of the simplex. The definition of γ_k in (1) implies that the maximum norm of error on edge $\mathbf{e}_k$ is simply $|\gamma_k|/4$. Using this, we get

$$|(\mathfrak{M}_\Delta \mathbf{e}_k, \mathbf{e}_k)| = 4\frac{\alpha_k}{|\gamma_k|}\|e_2\|_{L^\infty(\mathbf{e}_k)}.$$

Let us consider a mesh that is uniform in metric $\mathfrak{M}_\Delta$. For such a mesh, we immediately get the following equalities:

$$\frac{\alpha_1}{|\gamma_1|}\|e_2\|_{L^\infty(\mathbf{e}_1)} = \frac{\alpha_2}{|\gamma_2|}\|e_2\|_{L^\infty(\mathbf{e}_2)} = \cdots = \frac{\alpha_{n_d}}{|\gamma_{n_d}|}\|e_2\|_{L^\infty(\mathbf{e}_{n_d})}.$$

Thus, the optimal mesh equidistributes $\|e_2\|_{L^\infty(\mathbf{e}_k)}$ over all edges of each simplex Δ. It explains our choice for (4). Similar arguments are used to motivate the choice (6).

The choice (4) has another advantage. In spite of the local metric construction, we have approximate equality of edge length measured in different metrics $\mathfrak{M}_\Delta$ coming from simplexes Δ sharing the edge. In other words, the recovered cell-based metrics are globally consistent. This results is verified with numerical experiments in Section 4.1.

2.5 Error Estimates as Functions of N_h

The error equidistribution principle suggests to build meshes that are quasi-uniform in metric $\mathfrak{M}$, for the interpolation error, or in metric $\widetilde{\mathfrak{M}}$, for the gradient of the interpolation error. Let Ω_h and $\widetilde{\Omega}_h$ be simplicial meshes with N_h cells that balance the volume and perimeter of cells:

$$N_h^{-1}|\Omega|_{\mathfrak{M}_p} \simeq |\Delta|_{\mathfrak{M}_{\Delta,p}} \simeq |\partial\Delta|^d_{\mathfrak{M}_{\Delta,p}} \qquad \forall \Delta \in \Omega_h$$

and

$$N_h^{-1}|\Omega|_{\widetilde{\mathfrak{M}}_p} \simeq |\Delta|_{\widetilde{\mathfrak{M}}_{\Delta,p}} \simeq |\partial\Delta|^d_{\widetilde{\mathfrak{M}}_{\Delta,p}} \qquad \forall \Delta \in \widetilde{\Omega}_h,$$

where $a \simeq b$ means that $c\,a \le b \le C\,a$ with constants depending only on d and p. On such meshes, the following error estimates are held:

$$\|e\|_{L^p(\Omega)} = \left(\sum_{\Delta\in\Omega_h}\|e\|^p_{L^p(\Delta)}\right)^{\frac{1}{p}} \lesssim \left(\sum_{\Delta\in\Omega_h}|\Delta|^{1+\frac{2p}{d}}_{\mathfrak{M}_{\Delta,p}}\right)^{\frac{1}{p}} \lesssim |\Omega|^{\frac{1}{p}+\frac{2}{d}}_{\mathfrak{M}_p} N_h^{-\frac{2}{d}}$$

and

$$\|\nabla e\|_{L^p(\Omega)} = \left(\sum_{\Delta \in \widetilde{\Omega}_h} \|\nabla e\|^p_{L^p(\Delta)} \right)^{\frac{1}{p}} \lesssim \left(\sum_{\Delta \in \widetilde{\Omega}_h} |\Delta|^{1+\frac{p}{d}}_{\widetilde{\mathfrak{M}}_{\Delta,p}} \right)^{\frac{1}{p}} \lesssim |\Omega|^{\frac{1}{p}+\frac{1}{d}}_{\widetilde{\mathfrak{M}}_p} N_h^{-\frac{1}{d}}.$$

Thus, the $\mathfrak{M}_p$ (resp., $\widetilde{\mathfrak{M}}_p$)-quasi-uniform meshes provide asymptotically optimal rate for reduction of the interpolation error (resp., the gradient of the error).

3 Mesh Adaptation Algorithm

To build a continuous metric from a piecewise constant metric, we employ the method of shifts. For every node $\mathbf{a}_i$ in Ω_h, we define the superelement σ_i as the union of all d-simplices sharing $\mathbf{a}_i$. Then, to every node $\mathbf{a}_i$, we assign the metric with the largest determinant among all metrics associated with the superelement σ_i.

We use Algorithm 1 to build an adaptive mesh minimizing the L^p-norm of error or its gradient.

Algorithm 1. Adaptive mesh generation

1: Generate an initial mesh Ω_h, compute a piecewise constant metric $\mathfrak{M}_p$, and apply the method of shifts to get a continuous metric still denoted by $\mathfrak{M}_p$.
2: **loop**
3: Generate a $\mathfrak{M}_p$-quasi-uniform mesh Ω_h.
4: Recompute the metric $\mathfrak{M}_p$.
5: If Ω_h is $\mathfrak{M}_p$-quasi-uniform, then exit the loop.
6: **end loop**

To generate a $\mathfrak{M}$-quasi-uniform mesh, we use a sequence of local mesh modifications [2, 7, 17] that gradually increase the measure of mesh quasi-uniformity. The local modifications of mesh topology include edge swapping, node relocation, insertion and deletion. These operations are implemented in package `Ani2D` (sourceforge.net/projects/ani2d).

4 Numerical Results

4.1 Interpolation Problems

In this section, we demonstrate with numerical experiments that the recovered piecewise-constant metric is sufficiently 'smooth' and reflects anisotropic features of the interpolated function. Let $\mathcal{E}^0$ be the set of interior mesh edges.

In the two dimensional case, we define the measure of metric discontinuity as follows:

$$V(\mathfrak{M}) = \frac{1}{N(\mathcal{E}^0)} \sum_{\mathbf{e}\in\mathcal{E}^0} V_{\mathbf{e}}(\mathfrak{M}), \qquad V_{\mathbf{e}}(\mathfrak{M}) = \left| \frac{|||\mathbf{e}|||_{\mathfrak{M}_\Delta} - |||\mathbf{e}|||_{\mathfrak{M}_{\Delta'}}}{|||\mathbf{e}|||_{\mathfrak{M}_\Delta} + |||\mathbf{e}|||_{\mathfrak{M}_{\Delta'}}} \right|,$$

where $N(\mathcal{E}^0)$ is the number of interior edges and $\mathfrak{M}_\Delta$, $\mathfrak{M}_{\Delta'}$ are two triangles with the common edge e. Note that $V(\mathfrak{M})$ is zero for a continuous metric. For a sequence of refined shape-regular meshes and corresponding piecewise constant metrics approximating a continuous metric, $V(\mathfrak{M})$ is converging to zero.

In the first experiment, we calculate $V(\mathfrak{M})$ on a sequence of quasi-optimal meshes built with Algorithm 1. In the unit square $\Omega = [0,\, 1]^2$, we consider the analytical function proposed in [11]:

$$u(x,\, y) = \frac{(x-0.5)^2 - (\sqrt{10}y + 0.2)^2}{((x-0.5)^2 + (\sqrt{10}y + 0.2)^2)^2}.$$

The function has an anisotropic singularity at point $(0.5,\, -0.2/\sqrt{10})$ located outside the computational domain but close to its boundary. Table 1 shows that $V(\mathfrak{M})$ is roughly 0.1, i.e. the length of edge $\mathbf{e}$ varies roughly 20% when measured in metrics $\mathfrak{M}_\Delta$ and $\mathfrak{M}_{\Delta'}$ associated with this edge. Lack of convergence of $V(\mathfrak{M})$ to 0 as $N_h \to \infty$ may be related to the fact that the mesh is only quasi-uniform in metric $\mathfrak{M}$.

The L^∞-norm of the interpolation error is proportional to N_h^{-1}, while the L^∞-norm of its gradient is proportional to $N_h^{-0.5}$. Note that the meshes minimizing the interpolation error and its gradient are different (see Fig. 1). The figure indicates sharper features of the gradient of the error, which is the expected result.

In the second experiment, we consider the Texas-shape domain inscribed in $[-\frac{3}{2}; \frac{3}{2}]$ and shown in Fig 2. We consider the analytical function

$$u(x,\, y) = (x^2 y + y^3)/16^3 + \tanh(2(\sin(6y) - 3x)(\sin(6x) - 3y)) \qquad (15)$$

that has a spider-like distinguished feature highlighted by the mesh anisotropy. The results of numerical experiments collected in Table 2 confirm conclusions

Table 1. Experiment 1: convergence of the interpolation error and its gradient

	Interpolation error		Gradient of interpolation error	
N_h	$\|e\|_{L^\infty(\Omega)}$	$V(\mathfrak{M})$	$\|\nabla e\|_{L^\infty(\Omega)}$	$V(\mathfrak{M})$
1000	8.29e-2	0.122	5.41e+1	0.119
4000	2.36e-2	0.114	2.70e+1	0.097
16000	6.59e-3	0.115	1.42e+1	0.096
64000	1.83e-3	0.113	7.71e+0	0.099
rate	0.92		0.48	

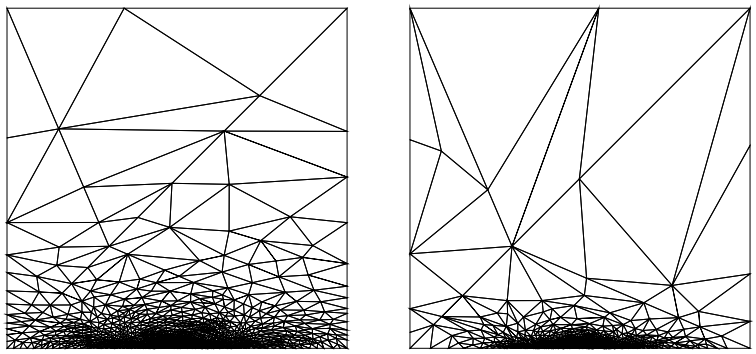

Fig. 1. Experiment 1: The adaptive meshes with roughly 2000 triangles minimizing the maximum norm of the interpolation error (left) and its gradient (right).

Table 2. Experiment 2: convergence of the interpolation error and its gradient.

	Interpolation error		Gradient of interpolation error	
N_h	$\|e\|_{L^\infty(\Omega)}$	$V(\mathfrak{M})$	$\|\nabla e\|_{L^\infty(\Omega)}$	$V(\mathfrak{M})$
1000	1.03e-1	0.197	1.75e-0	0.220
4000	2.09e-2	0.122	7.72e-1	0.146
16000	5.38e-3	0.098	3.76e-1	0.104
64000	1.39e-3	0.090	1.93e-1	0.090
rate	1.03		0.53	

that we made in the previous experiment. We observe the first-order convergence rate for the maximum norm of the error and the half-order convergence rate for the gradient of this error. The measure of metric discontinuity $V(\mathfrak{M})$ is slowly decreasing; however, its convergence to zero is questionable. Fig. 2 shows that the meshes minimizing the interpolation error and its gradient are different, which is the expected result.

Actual numerical values of $V(\mathfrak{M})$ cause slight but yet unpleasant instabilities in the adaptive process. We found numerically that the adaptation is more robust for a continuous tensor metric that provides faster convergence and results in a smoother mesh. That is why we use the method of shifts to generate of a continuous metric.

4.2 Applications to PDEs

In this section, we apply the developed methodology to adaptive solution of finite element problems. We consider problems with isotropic and anisotropic solutions.

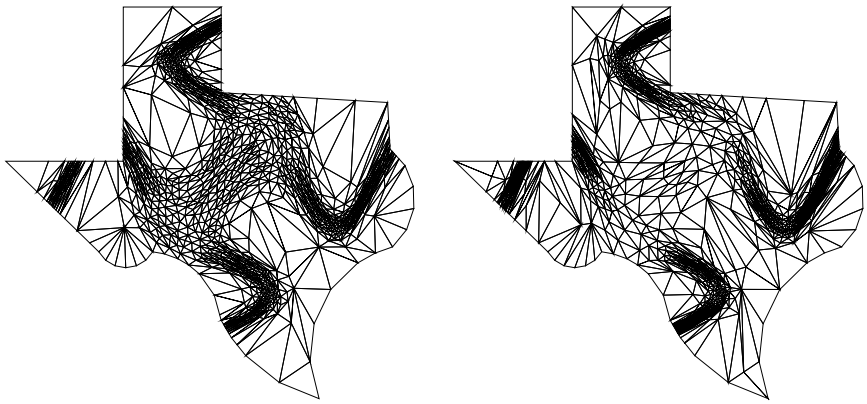

Fig. 2. Experiment 2: The adaptive meshes with roughly 2000 triangles minimizing the maximum norm of the interpolation error (left) and its gradient (right)

Hierarchical error estimates

We describe briefly a discretization error estimator based on enrichment of the linear finite element space with a space of piecewise quadratic finite element functions (bubbles) associated with edges of Ω_h [12]. The extended finite element problem results in a system of algebraic equations:

$$\begin{bmatrix} A_{LL} & A_{LQ} \\ A_{QL} & A_{QQ} \end{bmatrix} \begin{bmatrix} u_L \\ u_Q \end{bmatrix} = \begin{bmatrix} f_L \\ f_Q \end{bmatrix},$$

where subscripts L and Q stand for linear and quadratic terms.

Let u_L^* be an approximate solution of the original P_1 finite element problem $A_{LL}u_L^* = f_L$. We define the deviation $d_L = u_L - u_L^*$ and the discretization error $d_Q = u_Q$. They satisfy

$$\begin{bmatrix} A_{LL} & A_{LQ} \\ A_{QL} & A_{QQ} \end{bmatrix} \begin{bmatrix} d_L \\ d_Q \end{bmatrix} = \begin{bmatrix} r_L \\ r_Q \end{bmatrix}, \tag{16}$$

with

$$r_L = f_L - A_{LL}u_L^* \qquad \text{and} \qquad r_Q = f_Q - A_{QL}u_L^*.$$

The exact solution of (16) is too expensive. In order to estimate the discretization error d_Q, equation (16) is replaced with a simpler equation

$$\begin{bmatrix} A_{LL} & 0 \\ 0 & A_{QQ} \end{bmatrix} \begin{bmatrix} \tilde{d}_L \\ \tilde{d}_Q \end{bmatrix} = \begin{bmatrix} r_L \\ r_Q \end{bmatrix}. \tag{17}$$

Using a local finite element analysis, one can show that the diagonal matrix in (17) is spectrally equivalent to the matrix in (16). Therefore, the energy

norm of the discretization error d_Q can be estimated using the energy norm of $\tilde{d}_Q$. The matrix A_{QQ} is well-conditioned for shape-regular meshes; therefore, the vector $\tilde{d}_Q$ can be efficiently calculated with a simple conjugate gradient method.

The entry of vector $\tilde{d}_Q$ associated with an edge $\mathbf{e}_k$ of a simplex Δ plays the role of interpolation error γ_k in formula (1). Thus, we can use the above methodology to generate quasi-optimal meshes.

Problem with a point singularity

Let Ω be a unit disk with a radial cut. We consider the classical crack problem with the exact solution

$$u(r,\theta) = r^{1/4}\sin(\theta/4),$$

where $(r,\,\theta)$ are polar coordinates, $r > 0$ and $\theta \in [0,\,2\pi)$. The crack line S is defined by points $(r,\,0)$. We consider the following boundary value problem:

$$\begin{aligned} \Delta u &= 0 && \text{in} \quad \Omega \setminus S, \\ u &= \sin\frac{\theta}{4} && \text{on} \quad \partial\Omega \setminus S, \\ u &= 0 && \text{on} \quad S^+, \qquad \frac{\partial u}{\partial n} = 0 \qquad \text{on} \quad S^-, \end{aligned} \tag{18}$$

where S^+ and S^- denote the crack line when it is approached from regions $\theta \to +0$ and $\theta \to 2\pi$, respectively.

Table 3 demonstrates the half-order convergence of the gradient of the discretization error. A similar convergence is observed for the gradient of a finite element function $\tilde{d}_h$ corresponding to vector $\tilde{d}_Q$, which confirms the theory of hierarchical error estimates on shape-regular meshes. The difference in error values indicates that the constant of spectral equivalence of energy norms of d_Q and $\tilde{d}_Q$ is approximately 6.

This theory does not guarantee a similar connection between L^2-norms of these errors, which is also clear from the second and third columns in Table 3. For this norm, we have to use the finite element function d_h corresponding to d_Q; however, calculation of this function is rather expensive.

Problem with anisotropic singularities

Let Ω be the unit square $\Omega = (0,\,1)^2$. We consider the following boundary value problem:

$$\begin{aligned} -\mathrm{div}\,(\mathbb{K}\,\mathrm{grad}\,u) &= 1 \qquad \text{in} \quad \Omega, \\ u &= 0 \qquad \text{on} \quad \partial\Omega, \end{aligned}$$

where

$$\mathbb{K}(x,y) = \mathbb{R}_\theta^T \begin{bmatrix} 1 & 0 \\ 0 & 10^3 \end{bmatrix} \mathbb{R}_\theta, \qquad \theta = 250\,(x+y),$$

and $\mathbb{R}_\theta$ is the rotation matrix by angle θ. The analytical solution is unknown and the discretization error cannot be computed. However, some features

Table 3. Experiment 3: convergence of the discretization error and its gradient

	Discretization error		Gradient of discretization error	
N_h	$\|\tilde{d}_h\|_{L^2(\Omega)}$	$\|e\|_{L^2(\Omega)}$	$\|\nabla\tilde{d}_h\|_{L^2(\Omega)}$	$\|\nabla e\|_{L^2(\Omega)}$
1000	1.10e-3	7.44e-3	1.94e-2	1.17e-1
4000	2.84e-4	3.10e-3	1.01e-2	6.08e-2
16000	7.04e-5	1.30e-3	5.35e-3	2.96e-2
64000	1.76e-5	9.48e-4	2.62e-3	1.59e-2
rate	1.00	0.51	0.48	0.48

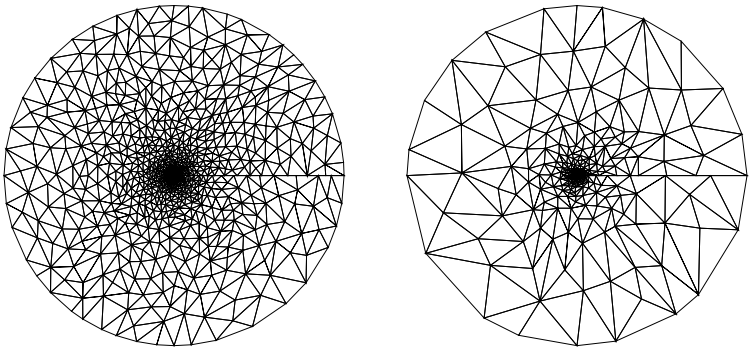

Fig. 3. Experiment 3: The adaptive meshes with roughly 2000 triangles minimizing the L^2-norm of the hierarchical error estimator (left) and its gradient (right)

Table 4. Experiment 4: convergence of the hierarchical error estimators $\tilde{d}_h$, d_h and their gradients

	Discretization error		Gradient of discretization error	
N_h	$\|\tilde{d}_h\|_{L^2(\Omega)}$	$\|d_h\|_{L^2(\Omega)}$	$\|\nabla\tilde{d}_h\|_{L^2(\Omega)}$	$\|\nabla d_h\|_{L^2(\Omega)}$
1000	4.98e-6	5.55e-3	1.88e-4	6.52e-4
4000	1.48e-6	3.02e-3	1.16e-4	3.52e-4
16000	3.88e-7	1.82e-3	5.94e-5	1.67e-4
64000	9.87e-8	1.03e-3	2.94e-5	9.07e-5
rate	0.95	0.40	0.45	0.48

of the solution can be extracted from the mesh structure shown in Fig. 4. Table 4 shows that the gradient of hierarchical edge-based a posteriori error estimator, $\|\nabla\tilde{d}_h\|_{L^2(\Omega)}$, correlates with $\|\nabla d_h\|_{L^2(\Omega)}$ even on anisotropic meshes. Similarly to the previous experiment, the L^2-norms of these estimators exhibit different behavior.

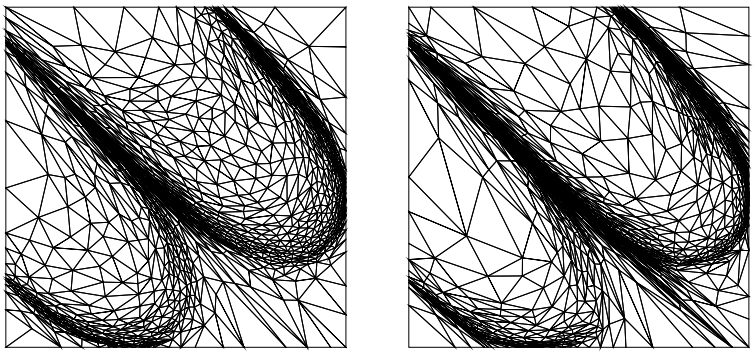

Fig. 4. Experiment 4: The adaptive meshes with roughly 2000 triangles minimizing the L^2-norm of the hierarchical error estimator $\tilde{d}_h$ (left) and its gradient (right)

5 Conclusion

We presented a new technology for generating meshes minimizing the interpolation and discretization errors or their gradients. The cornerstone of this methodology is construction of a space metric from edge-based error estimates. For the interpolation error, these estimates were computed explicitly. For the discretizations error, we used the hierarchical error estimators based on enrichment of the linear finite element space with quadratic bubble functions associated with mesh edges. We proved and verified with numerical experiments, that for a mesh with N_h triangles, the error is proportional to N_h^{-1} and the gradient of this error is proportional to $N_h^{-1/2}$, which are optimal asymptotics.

Acknowledgments. Research of the third author has been supported partially by the RFBR project 08-01-00159-a.

References

1. Agouzal, A., Vassilevski, Y.: Minimization of gradient errors of piecewise linear interpolation on simplicial meshes. Submitted to SIAM J. Numer. Anal. (2008)
2. Agouzal, A., Lipnikov, K., Vassilevski, Y.: Adaptive generation of quasi-optimal tetrahedral meshes. East-West J. Numer. Math. 7, 223–244 (1999)
3. Agouzal, A., Lipnikov, K., Vassilevski, Y.: Generation of quasi-optimal meshes based on a posteriori error estimates. In: Brewer, M., Marcum, D. (eds.) Proceedings of 16th International Meshing Roundtable, pp. 139–148. Springer, Heidelberg (2007)
4. Agouzal, A., Lipnikov, K., Vassilevski, Y.: Hessian-free metric-based mesh adaptation via geometry of interpolation error. Comp. Math. Math. Phys. 49(11) (to appear, 2009)

5. Ait-Ali-Yahia, D., Habashi, W.G., Tam, A., Vallet, M.-G., Fortin, M.: Directionally adaptive methodology using an edge-based error estimate on quadrilateral grids. Inter. J. Numer. Meth. Fluids 23(7), 673–690 (1996)
6. Bono, G., Awruch, A.M.: An adaptive mesh strategy for high compressible flows based on nodal re-allocation. J. Brazilian Soc. Mech. Sci. Engr. 30(3), 189–196 (2008)
7. Buscaglia, G.C., Dari, E.A.: Anisotropic mesh optimization and its application in adaptivity. Inter. J. Numer. Meth. Engrg. 40, 4119–4136 (1997)
8. Chen, L., Sun, P., Xu, J.: Optimal anisotropic meshes for minimizing interpolation errors in L^p-norm. Mathematics of Computation 76, 179–204 (2007)
9. Ciarlet, P., Wagschal, C.: Multipoint Taylor formulas and applications to the finite element method. Numer. Math. 17, 84–100 (1971)
10. Ciarlet, P.: The finite element method for elliptic problems. North-Holland, Amsterdam (1978)
11. D'Azevedo, E.: Optimal triangular mesh generation by coordinate transformation. SIAM J. Sci. Stat. Comput. 12, 755–786 (1991)
12. Deuflhard, P., Leinen, P., Yserentant, H.: Concepts of an adaptive hierarchical finite element code. IMPACT 1, 3–35 (1989)
13. Frey, P.J., Alauzet, F.: Anisotropic mesh adaptation for CFD computations. Comput. Meth. Appl. Mech. Eng. 194, 5068–5082 (2005)
14. Huang, W.: Metric tensors for anisotropic mesh generation. J. Comp. Physics. 204, 633–665 (2005)
15. Lipnikov, K., Vassilevski, Y.: Parallel adaptive solution of 3D boundary value problems by Hessian recovery. Comput. Meth. Appl. Mech. Eng. 192, 1495–1513 (2003)
16. Tichomirov, V.M.: The widths of sets in functional spaces and theory of optimal approximations. Uspehi Matem. Nauk 15(3), 81–120 (1960)
17. Vassilevski, Y., Lipnikov, K.: Adaptive algorithm for generation of quasi-optimal meshes. Comp. Math. Math. Phys. 39, 1532–1551 (1999)
18. Vassilevski, Y., Agouzal, A.: An unified asymptotic analysis of interpolation errors for optimal meshes. Doklady Mathematics 72, 879–882 (2005)
19. Zhu, J.Z., Zienkiewicz, O.C.: Superconvergence recovery technique and a posteriori error estimators. Inter. J. Numer. Meth. Engrg. 30, 1321–1339 (1990)